Acta Crystallographica Section D
Biological Crystallography
ISSN 0907-4449

Comparative analysis of space-grown and earth-grown crystals of an aminoacyl-tRNA synthetase: space-grown crystals are more useful for structural determination

Joseph D. Ng,[a,b] Claude Sauter,[a]† Bernard Lorber,[a] Natalie Kirkland,[b] John Arnez[c]‡ and Richard Giegé[a]*

[a]Département 'Mécanismes et Macromolécules de la Synthèse Protéique et Cristallogenèse', UPR 9002, Institut de Biologie Moléculaire et Cellulaire du CNRS, 15 Rue René Descartes, F-67084 Strasbourg CEDEX, France, [b]Laboratory for Structural Biology and Department of Biological Science, University of Alabama in Huntsville, Huntsville, AL 35899, USA, and [c]UPR 9004, Institut de Génétique et de Biologie Moléculaire et Cellulaire, 1 Rue Laurent Fries, BP 163, F-67404 Illkirch Cedex, France

† Present address: European Molecular Biology Laboratory (EMBL), Meyerhofstrasse 1, Postfach 10.22.09, D-69012 Heidelberg, Germany.
‡ Present address: Albert Einstein College of Medicine, Bronx, NY 10461, USA.

Correspondence e-mail: r.giege@ibmc.u-strasbg.fr

Received 25 August 2001
Accepted 18 February 2002

PDB Reference: space-grown aspartyl-tRNA synthetase-1, 1l0w, r1l0wsf.

Protein crystallization under microgravity aims at benefiting from the quasi-absence of convection and sedimentation to favor well ordered crystal nucleation and growth. The dimeric multidomain enzyme aspartyl-tRNA synthetase from *Thermus thermophilus* has been crystallized within dialysis reactors of the Advanced Protein Crystallization Facility in the laboratory on earth and under microgravity aboard the US Space Shuttle. A strictly comparative crystallographic analysis reveals that the crystals grown in space are superior in every respect to control crystals prepared in otherwise identical conditions on earth. They diffract X-rays more intensely and have a lower mosaicity, facilitating the process of protein structure determination. Indeed, the electron-density map calculated from diffraction data of space-grown crystals contains considerably more detail. The resulting three-dimensional structure model at 2.0 Å resolution is more accurate than that produced in parallel using the data originating from earth-grown crystals. The major differences between the structures, including the better defined amino-acid side chains and the higher order of bound water molecules, are emphasized.

1. Introduction

The crystallization of biological macromolecules has been repeatedly investigated in microgravity environments within the last two decades after lysozyme was observed to yield larger crystals in space than on earth (Littke & John, 1984). Many biological macromolecules, ranging in size from less than 100 amino-acid long polypeptides to large high-molecular weight and multi-macromolecular assemblies, have been crystallized in terrestrial orbit to take advantage of the very weak convection and sedimentation existing in quasi-weightlessness. Despite the variety of protein samples that were assayed in space, success has been limited. One reason is the low number of crystallization assays set up in space for each molecule; they represent only a small fraction of those tested in the same time span in earth-based laboratories. Another is that the optimal conditions for crystal growth in microgravity may differ from those found on earth (McPherson, 1997; Kundrot *et al.*, 2000). The improvement in quality of microgravity-grown crystals has been correlated with the number of experimental iterations to find optimal conditions (Kundrot *et al.*, 2000). In a number of cases, larger crystals diffracting X-rays with a superior intensity and to a higher resolution were produced (*e.g.* DeLucas *et al.*, 1989;

Wardell *et al.*, 1997; Boggon *et al.*, 1998). Over the years, it has been concluded that microgravity has a positive effect on the production of protein crystals (*e.g.* DeLucas *et al.*, 1989, 2000; Snell *et al.*, 1995; McPherson, 1996; Ng *et al.*, 1997; Carter *et al.*, 1999; Declercq *et al.*, 1999; Lorber *et al.*, 1999; Moore *et al.*, 1999; Borgstahl *et al.*, 2001). This conclusion is based on a comparison of the properties of crystals returning from space with those of the best crystals of the same molecule ever grown on earth, be it under different conditions, in another experimental setup or using another technique.

The longstanding question is whether the quality improvement seen in the crystals that are prepared under microgravity can actually be more useful for structure determination and lead to better structures than crystals that are prepared on earth. This is crucial, since the ultimate goal is to obtain macromolecular structure models at the highest resolution. In the case of the low-molecular weight and monomeric model protein lysozyme, high-resolution structures could be derived from microgravity-grown crystals (Vaney *et al.*, 1996; Sauter *et al.*, 2001). Comparative studies have pointed out that crystals from space can yield better structural data: slight improvements in the bound solvent (Dong *et al.*, 1999) as well as higher resolution and lower isotropic *B* factors (Carter *et al.*, 1999) were observed. Presently, additional experimentation is required to generalize the applicability of the approach to representative functional biomacromolecules, including high-molecular-weight and multisubunit enzymes.

Here, we report a comparative crystallographic analysis that was conducted on the enzyme aspartyl-tRNA synthetase 1 (AspRS-1) from the thermophilic eubacterium *Thermus thermophilus*, crystals of which have been grown under microgravity on the US Space Shuttle during the STS-78 mission. AspRS-1 is a homodimer of 122 kDa with a subunit encompassing 580 amino acids (Becker *et al.*, 1997). It catalyzes the aspartylation of $tRNA^{Asp}$ in the process of translating genetic information. The three-dimensional structure previously solved at 2.5 Å resolution highlights its modular and dynamic character: each subunit possesses the three domains that are common to all known AspRSs and two prokaryote-specific modules (Delarue *et al.*, 1994). This multidomain and multisubunit enzyme was crystallized on earth and in space within dialysis reactors of the Advanced Protein Crystallization Facility (APCF). Our rigorous comparison shows that the intrinsic order of the space-grown crystals, which contain as much as 62%(*v*/*v*) solvent, is enhanced with respect to that of control crystals prepared on earth under otherwise identical conditions. This conclusion is based on the higher intensity of the X-ray diffraction, the lower mosaic spread of the reflection profiles and the higher quality electron-density map computed from the diffraction data. As a consequence, a better three-dimensional structure model at 2.0 Å resolution covering the entire polypeptide chain could be obtained from the analysis of space-grown crystals. Major differences from the model derived from control diffraction data, including the well defined side chains of amino acids and the greater number of ordered water molecules, are emphasized.

2. Materials and methods

2.1. Protein preparation

The eubacterium *T. thermophilus* possesses two aspartyl-tRNA synthetases differing in sequence and catalytic activity (Becker *et al.*, 1997). The present study deals with the former enzyme (termed AspRS-1; Swiss-Prot accession code P36419). It was expressed in *Escherichia coli* and could be enriched easily because it is heat tolerant and remains soluble while most proteins of the host bacterium are denatured at 343 K. The synthetase was further purified using two chromatographic steps as described by Poterszman *et al.* (1993) with slight modifications. The final preparation was >90% homogeneous as estimated by SDS–PAGE (results not shown).

2.2. Crystallization conditions and apparatus

Earth-grown and space-grown AspRS-1 crystals were obtained at 293 ± 0.5 K in 67 µl chambers of four APCF dialysis reactors (Bosch *et al.*, 1992) using conditions adapted from those described for the vapor-diffusion technique (Delarue *et al.*, 1994; Ng *et al.*, 1996). Crystals were grown from protein solutions at 20 mg ml^{-1} containing 2.2 *M* ammonium sulfate, 25 m*M* Tris–HCl pH 7.5, 10 m*M* EDTA, 1 m*M* DTT and 0.01%(*m*/*v*) PMSF. Crystallization under microgravity took place aboard the NASA space shuttle during the 16 d STS-78 mission designated the 'Life Microgravity Spacelab (LMS)'. The dialysis reactors consist of two quartz-glass blocks separated by a semipermeable membrane (Spectra/Por1, molecular-weight cutoff 6–8 kDa). The upper block contains the protein solution and the lower block the precipitant solution. A cylindrical quartz plug containing the second solution separates both chambers. In microgravity, a 90° rotation of the plug brought the contents of all chambers into contact. The reverse operation was performed a few hours before the end of the microgravity session prior to landing. Control experiments have been conducted in parallel in the same type of reactors and with the same solutions. All reactors underwent identical transport and handling conditions during the pre-launch and post-landing phases of the mission. Both control and space experiments were activated for a total duration of 338 h.

2.3. X-ray diffraction analysis

Crystals were mounted in 3 mm quartz capillaries (Charles Supper Co., Natick, MS, USA) as described by McPherson (1982) and analyzed at 293 K. The dimensions of the crystals were measured under a standard optical low-power microscope equipped with a microruler.

X-ray diffraction data sets were collected on beamline X11 at the EMBL Outstation Hasylab at DESY (Hamburg, Germany) using a MAR Research imaging plate. All crystals were of orthorhombic habit and belonged to space group $P2_12_12_1$, with unit-cell parameters a = 61.4, b = 156.1, c = 177.3 Å. For the purpose of comparison, complete diffraction data sets were recorded on crystals having the same size and volume under standardized conditions. The crystal-to-

detector distance was 250 mm, the exposure time was approximately 30 s (in dose mode), the oscillation angle was 0.5° and the wavelength was 0.91 Å. The collected data were indexed and reduced with the programs *DENZO* and *SCALEPACK* (Otwinowski & Minor, 1997). Two crystals from each population of earth-grown and space-grown crystals were averaged and used for the subsequent structural analyses. The processing statistics for each data set are given in Table 1.

Crystal mosaicity was evaluated from the rocking width of selected reflections (Helliwell, 1988) using the method of Ferrer & Roth (1998). Reflection profiles representing intensity *versus* oscillation angle were recorded using a CCD detector on beamline D2AM at ESRF (Grenoble, France). The X-ray bending-magnet source critical energy was 19.5 keV with a focused beam of 0.3 mm diameter at the sample, with a maximum vertical divergence of 0.15 mrad and a maximum horizontal divergence of 9.0 mrad (Ferrer *et al.*, 1996). Full beam intensity was $\sim 10^{11}$ photons s^{-1}, with an energy resolution $\delta\lambda/\lambda \simeq 10^{-4}$. Direct measurements were performed by indexing reflections over an oscillation range of 0.5° and subsequently over 0.2° at steps of 0.003° with 10 s exposures. Data were processed with *XDS* and intensities quantified with *MARVIEW* (Kabsch, 1988). Reflections were measured in the vertical plane with respect to the incident beam, so that a fully recorded reflection can be expressed simply as $\varphi_\rho = \gamma + \eta + (\delta\lambda/\lambda)\tan\theta$, where φ is the reflecting range, γ is the mean divergence in the plane defined by the direct and the diffracted beams, η is the crystal sample mosaicity, λ is the average wavelength of the X-ray beam and θ is the Bragg angle of the reflection (Colapietro *et al.*, 1992; Snell *et al.*, 1995). The values of γ and $\delta\lambda/\lambda$ were minimized by considering only reflections located in the vertical plane, including the incident beam and those at low resolution. Data were not corrected for Lorentz broadening; however, the instrument resolution-function value (IRF) was deconvoluted before the full-width-at-half-maximum (FWHM) of the profiles was determined.

Table 1
Data-processing statistics for earth-grown and space-grown AspRS-1 crystals.

Diffraction data were collected from crystals of approximately the same size (the smallest crystals prepared in space and the largest ones prepared on earth were used). Two crystals were used in each category.

	Earth	Space
No. of crystals	2	2
Resolution range (Å)	12.0–2.0	12.0–2.0
No. of observations	304251	320200
No. of unique reflections	111417	100854
Completeness (%)		
Overall	96.7	93.3
Lowest shell†	83.1	85.5
Highest shell‡	97.2	95.3
$R_{\rm merge}$§ (%)		
Overall	4.7	5.7
Lowest shell †	2.5	2.3
Highest shell‡	22.6	23.5
$\langle I/\sigma(I)\rangle$		
Overall	15.24	17.30
Lowest shell†	22.81	43.78
Highest shell‡	3.10	3.16

† 12.00–4.25 Å. ‡ 2.07–2.00 Å. § $R_{\rm merge} = \sum(I - \langle I\rangle)/\sum\langle I\rangle$.

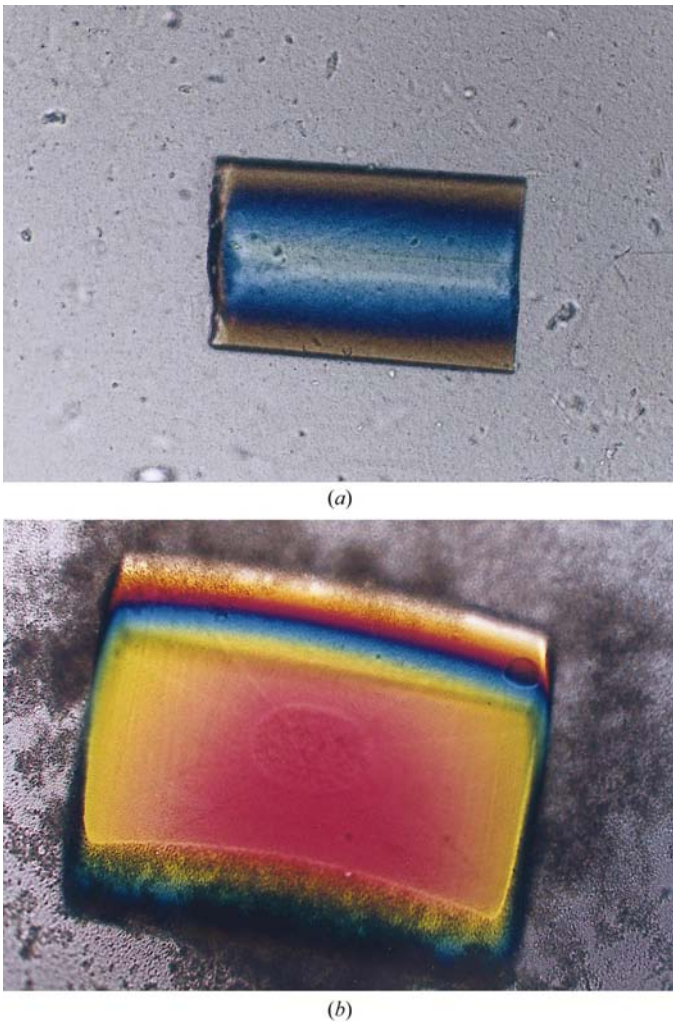

Figure 1
Earth-grown (*a*) and space-grown (*b*) crystals of AspRS-1. The photographs are on roughly the same scale with crystal dimensions of 1.75 × 1.25 × 0.65 mm and 3.0 × 1.75 × 1.0 mm, respectively.

2.4. Structure determination and refinement

The starting model for the refinement of the earth-grown and space-grown crystal structures was taken from available atomic coordinates (Delarue *et al.*, 1994) without any water molecules. Only reflections common to the data sets of both types of crystals were used in the 12–2.0 Å resolution range and the same sets of reflections (5%) were randomly selected for $R_{\rm free}$ testing (Brünger, 1992). The AspRS-1 model was then refined using the *CNS* package (Brünger *et al.*, 1998), with rigid-body refinement followed by simulated-annealing refinement rounds using bulk-solvent and anisotropic *B*-factor corrections. The structure model was further rebuilt with *O* (Kleywegt & Jones, 1997). The same refinement–rebuilding procedure was applied to both structures.

3. Results

In this work, our aim was to investigate whether differences arising from microgravity in the quality of protein crystals correlate with differences in the quality of the electron-density maps. Consequently, the usefulness of the protein crystals is determined by how well they can be used to provide an interpretable electron-density map for model building and refinement. Thus, two sets of crystals, those obtained in the laboratory and in the Space Shuttle (referred here to 'earth' and 'space' crystals, respectively), were analyzed in detail in parallel. Emphasis was placed on conducting strictly comparative experiments and, in particular, on computing density maps using exactly the same sets of Bragg reflections for both types of crystals.

3.1. Crystallization in space *versus* on earth

Microgravity and earth crystallization assays have yielded a small number of nuclei. Only two or three crystals grew in each reactor chamber from a precipitate which formed when supersaturation increased once the salt had diffused into the protein solution (Ng *et al.*, 1996). A total of nine crystals were obtained from four reactors activated under microgravity. Their average volume was estimated to be 3.4 mm^3 and the dimensions of the largest crystal were 3.0 × 1.75 × 1.0 mm (Fig. 1). In contrast, over 24 crystals were grown in the ground-control reactors, having an average volume of about 1.1 mm^3. The largest earth-grown crystal measured 1.75 × 1.25 × 0.65 mm. Crystals grown under microgravity had a larger volume on average and were visually observed to have less surface defects. This observation is consistent with those reported by other investigators on space-grown crystals (some examples include Koszelak *et al.*, 1995; Moore *et al.*, 1999; DeLucas *et al.*, 2000; Borgstahl *et al.*, 2001 and references therein). Two crystals representing those grown on earth and two crystals obtained in space were used for the subsequent X-ray analysis. All crystals analyzed had approximately the same volume of 1.2 mm^3.

3.2. Diffraction properties of space-grown crystals

Diffraction data sets with a completeness of >90% have been collected. Their data-reduction analyses statistics are listed in Table 1. A comparison of equivalent reflections belonging to both earth and space data sets indicated that intensities from the latter are superior by as much as 40%, although the average I/σ and $R_{\rm merge}$ values defined essentially the same diffraction limit (Fig. 2). On the other hand, the FWHMs of reflections measured from space crystals are on average more than four times smaller than those of earth crystals. We have examined over 20 reflections, but only those that were not affected by radiation damage were compared. FWHM measurements were performed for 12 reflections at 4 Å resolution. Student's *t* test was performed on the microgravity and ground mosaicity values, showing normal distributions having unequal variance in the two populations. The microgravity and the earth data are statistically different from each other at the 95% confidence interval (t = 15.2, sdev = 8.7) for mean 11.4–21.9 and 65.7–76.1 for space and earth data, respectively. The mean values and standard deviations are listed in Table 2.

Table 2
Mosaicity characteristics of earth-grown and space-grown AspRS-1 crystals.

	Earth	Space
No. of crystals	2	2
No. of reflections	12	12
Mean FWHM (mdeg)	70.9	16.7
Standard deviation on mean FWHM (mdeg)	10.4	6.6

Rocking curves exemplifying three representative reflections from earth and space crystals are displayed in Fig. 3. The most striking observation was the very broad and rough mosaic profiles for the reflections measured from earth crystals compared with the more narrow and sharp profiles from those of space crystals. The broad mosaic spread of earth crystal reflections was most notable during data processing, rendering the earth data set more difficult to index and to reduce. The higher diffraction intensity of the space-grown crystal most likely results from the simultaneous reduction of diffuse scattering (decreasing the background signal) and an increase in internal order. These features were also observed for other microgravity-grown crystals (Snell *et al.*, 1995; Harp *et al.*, 2000; Borgstahl *et al.*, 2001).

The enhanced order within the space-grown crystals led to lower mosaic spread, *i.e.* sharper diffraction profiles. The earth crystals may have an accumulation of defects, including the build-up of impurities in the growth solution. Since the space crystals may still be growing, there may be less disorder and

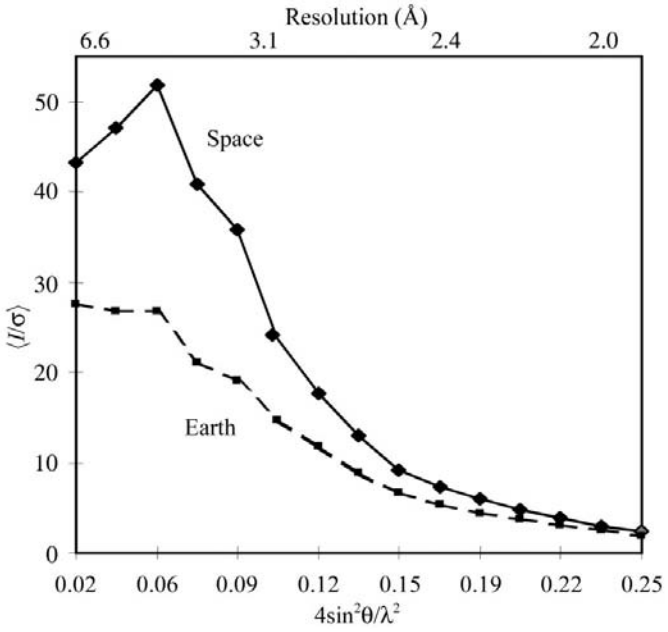

Figure 2
Graph of the diffraction intensities ($\langle I/\sigma\rangle$, average intensity over estimated error ratio) *versus* resolution for AspRS-1 crystals. Space-grown crystals showed as much as 40% more intensity in $\langle I/\sigma\rangle$ relative to earth-grown crystals in the resolution range analyzed.

less stress in the crystalline lattice. The improved mosaicity of the space-grown crystals is likely to result in improved data quality under suitably finely collimated beam conditions. Overall, by the current standards of crystallography, space AspRS-1 crystals are of higher order than earth crystals. Similar results were reported for crystals of low molecular-weight monomeric proteins such as lysozyme (Snell *et al.*, 1995; Otálora *et al.*, 1999), thaumatin (Ng *et al.*, 1997; Lorber *et al.*, 1999) and collagenase (Broutin-L'Hermite *et al.*, 2000), which all contain about 40–50%(*v*/*v*) solvent.

3.3. Quality of electron-density maps

Initial electron-density maps have been calculated using diffraction data collected from earth and space crystals as previously described. Each data set was collected from two crystals. The respective $2F_o - F_c$ maps (2 Å) were compared after one cycle of rigid-body minimization and simulated-annealing refinement against the original model derived from earth crystals (Delarue *et al.*, 1994). Significant differences are observed in the quality of the electron-density map that are distributed over the entire AspRS and not just located in particular parts of the subunits. Overall, the polypeptide backbone much more easily fits the electron density observed with space data. Some striking differences are shown in the close-up views of the maps displayed in Fig. 4. For instance, the side chain of Tyr6 is clearly visible within the map of the space crystals, while it cannot be seen in that of the control crystals (Fig. 4, top panels). Tyr6 is in the N-terminal domain of the synthetase that recognizes the anticodon of $tRNA^{Asp}$ and is subjected to a rigid-body movement upon this binding (Briand *et al.*, 2000). Other examples are the pyrrolidine ring of Pro169 and the aromatic ring of Phe170 (Fig. 4, middle panels).

Table 3
Model-refinement statistics for earth-grown and space-grown AspRS-1 crystals.

	Earth	Space
Refinement		
Resolution range (Å)	12.0–2.0	12.0–2.0
R_{free} (%)	25.8	25.0
R factor (%)	23.3	21.9
No. of reflections used†	81861	81861
Number of H_2O molecules‡	164	183
Luzzati coordinate error	0.271	0.255
Cross-validated coordinate error	0.17	0.16
Mean B factors (Å^2)	45.4	41.0
Ramachandran plot details§		
Residues in favoured regions (%)	87.5	88.0
Residues in additional allowed regions (%)	11.7	11.1
Residues in generously allowed regions (%)	0.7	0.7
Residues in disallowed regions (%)	0.1	0.2

† Only the reflections (~80%) common to both data sets with $I/\sigma(I) > 3$ were used to refine the AspRS models. ‡ In the space-grown crystals, the solvent is more ordered in the direct neighbourhood of the AspRS surface (closer than 3.4 Å). The 85 water molecules that are conserved between the two structures have average B factors of 31.5 and 35.7 Å^2 in microgravity and earth controls, respectively. § Calculated with *PROCHECK* (Laskowski *et al.*, 1993) for 986 non-glycine and non-proline residues.

Finally, Trp351 and Phe388, two residues belonging to the helical strand E4 in the extra-domain inserted between AspRS motifs 2 and 3, have a weaker density in the map of control crystals grown on earth (Fig. 4, bottom panels).

3.4. Model accuracy and bound water molecules

Successive refinements of the atomic models using diffraction data originating from earth and space crystals were performed using identical protocols. While refining the earth model, it appeared that the data were not sufficient to reach convergence quickly. Therefore, the final space model was

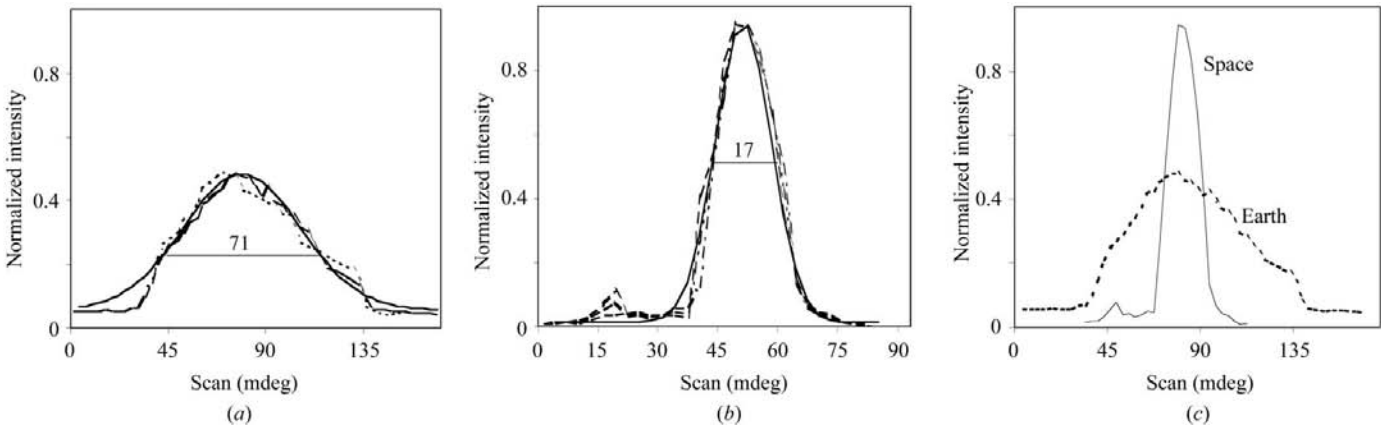

Figure 3
Intensity profiles of three representative reflections (14 8 9), (4 33 −13) and (14 5 −7) at 4 Å were each evaluated from (*a*) an earth-grown and (*b*) a space-grown AspRS-1 crystal. Reflections were obtained in the vertical diffraction plane such that the rotation axis was horizontal and perpendicular to the X-ray beam. Each set of reflection profiles for earth-grown and space-grown crystals were averaged and Gaussian fits of the sets of profiles were calculated (solid lines). The Gaussian plots were fitted to the principal peaks in which the full-width-at-half-maximum values (FWHMs) were evaluated. The FWHM of a Gaussian fit for each profile was measured and its value deconvoluted out by the instrument resolution-function value (IRF = 9 mdeg). FWHM values are indicated by short horizontal lines in the profiles and show that the space-grown crystals are about four times less mosaic than the earth-grown crystals. The intensities shown are normalized and the actual peak intensities measured to 85 236 counts per 0.1 s for the space crystal. In contrast, the spot intensities corresponding to the same reflections for the earth crystal were approximately two times smaller. (*c*) A relative comparison of the averaged mosaicity profiles of an earth-grown and a space-grown crystal for the same reflection. Profiles are centered on their maximum of intensity.

used to facilitate the model building. This enabled us to reconstruct the N- and C-terminal strands, the surface loops, the side chains and the addition of water molecules.

The quality of the final models has been estimated by three approaches. Firstly, the coordinates were used to assess the accuracy of each structure by evaluating the degree of chemically sensible local environments, the statistical distribution of atomic distances, the deviation from standard atomic volumes and the atomic solvation preferences. As a result, the local structures obtained from microgravity-grown crystals show slight improvements in geometry. Secondly, conventional *R* factors and coordinate errors were calculated for both earth and space structures. A 1.3% improvement in the overall *R* factor and a lower coordinate error (as reflected by the Luzzati and cross-validation analysis) confirmed that the model derived from space crystals is of better quality (Table 3).

Finally, the visibility of solvent molecules contributing to the global accuracy of the AspRS structure was considered using the difference density quality assessment (*DDQ*; van den Akker & Hol, 1999), which confers a score on each protein crystal structure, a high *DDQ* score representing a high accuracy. This method relies on the accuracy of the information in a so-called 'hydrated difference Fourier map' where the optimal positions of water peaks indicate the correctness of the positions of the protein residues surrounding the water molecules. The height of the water peaks is reflected on the quality of phases and thus the overall correctness of the structure. The overall *DDQ* statistics for the earth and space structures were DDQ-W = 2.3, DDQ-R = 5.5

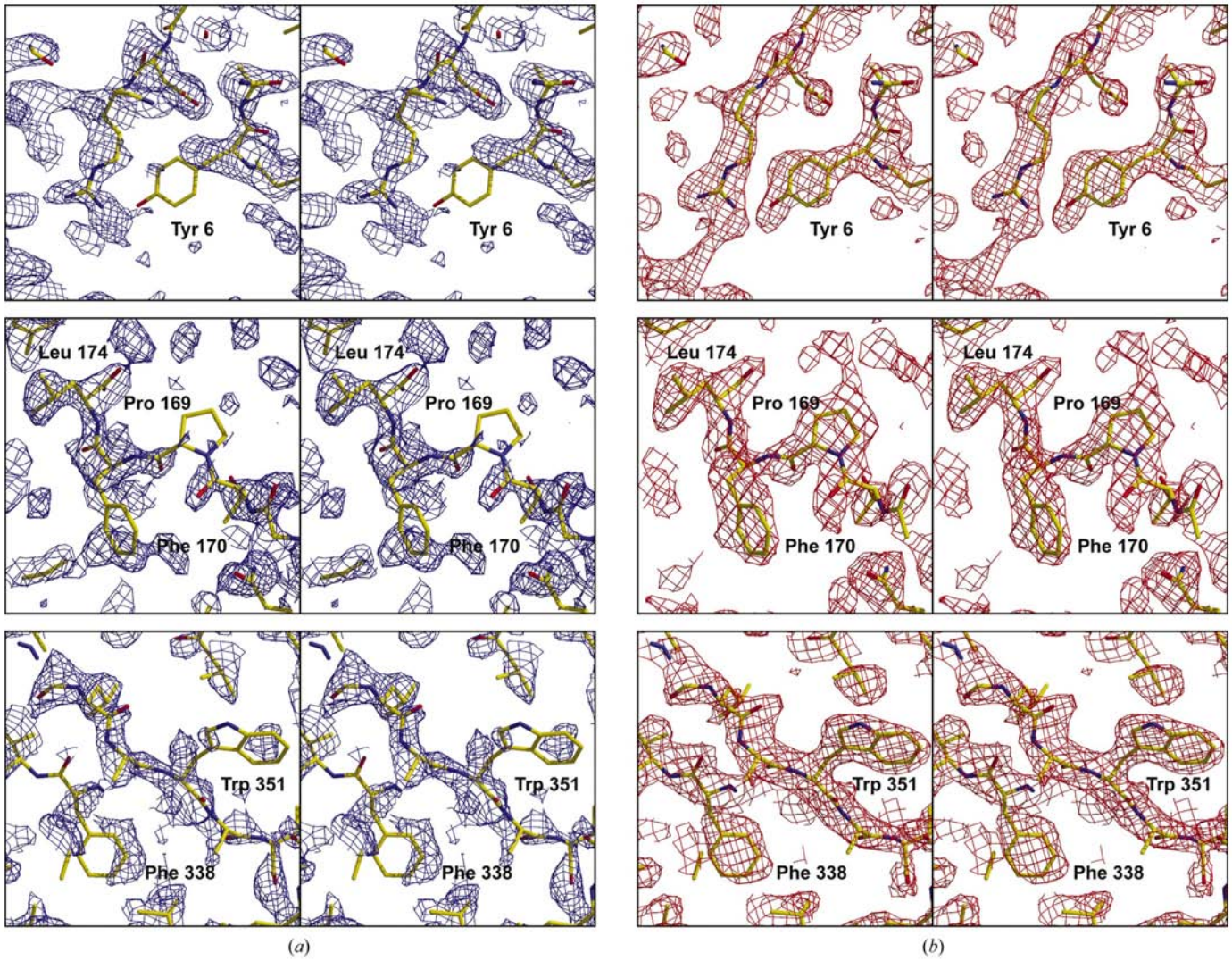

Figure 4
Comparative initial $2F_o - F_c$ electron-density maps (contoured at 2σ) calculated from (*a*) earth-grown and (*b*) space-grown crystal data. Three different regions of the synthetase monomer are displayed which illustrate the difference in quality between the data collected from earth-grown and space-grown crystals. The top panels emphasize residue 6 proximal to strands S1 to S4 of the N-terminal domain forming the oligonucleotide-binding fold that binds the anticodon of the tRNA. Middle panels emphasize residues 169, 170 and 171 in strand A2 of the antiparallel β-sheet forming the catalytic domain. Bottom panels emphasize residues 351 and 388 in the helical strand E4 of the extra domain. Residues and strands are referenced as in an earlier reported model (Delarue *et al.*, 1994). The figure was prepared using *SETOR* (Evans, 1993).

and DDQ-W = 8.3, DDQ-R = 12.4, respectively (DDQ-W values correspond to the correctness of water-peak positions, while DDQ-R values correspond to the global structure correctness).

Since fluid convection-driven motion around the crystallizing protein depends on the level of gravity, the global degree of order of the bound water molecules may vary under different growth environments. The identified solvent positions show more deviation from ideal distances for a substantial number of amino-acid main and side chains in the model derived from earth-grown crystals than in the space model. The deviations highlighted by the *DDQ* analysis could not be detected using a different validation procedure such as measuring the real-space correlation coefficient (Jones *et al.*, 1991). As a result, 164 and 183 water molecules were identified in the asymmetric unit of earth and space crystals, respectively. Similar observations have been made on space crystals of two small monomeric proteins. The microgravity structures of lysozyme and phospholipase A_2 show an extended network of 104 and 141 hydrogen-bonded water molecules, compared with only 92 and 97 in models derived from earth crystals prepared under otherwise identical conditions (Dong *et al.*, 1999, 2000).

This greater number of visible solvent atoms may well be correlated with a reduction of the mean *B* factor, which is only 41 Å^2 in microgravity-grown AspRS-1 crystals compared with 45 Å^2 for the earth controls (Table 3). This means that at the level of the protein, the atomic displacement parameters are reduced in a low-gravity environment, as reported in the case of several other proteins including isocitrate lyase, elastase, γ-interferon, malic enzyme and proline isomerase (Moore *et al.*, 1999).

4. Discussion

The process of protein crystallogenesis is influenced by many parameters (McPherson, 1999; Ducruix & Giegé, 1999). In the gravitational field of the earth, crystal growth generates variations in solution composition and microcrystals settle as soon as they reach a critical size. Both phenomena create differences in solution density and lead to fluid movements that end in mixing. In the absence of gravity, nuclei deplete the steady and immobile solution surrounding them of soluble macromolecules when they grow. Such protein-depleted zones have been visualized using interferometric methods (Otálora *et al.*, 2001). Under these conditions, crystal growth is gradually limited by the diffusion of the macromolecules approaching the surface of the crystal faces rather than by the incorporation into the latter.

A 10^3–10^5-fold reduction in gravity provides a quiescent medium in which the ordered arrangement of the AspRS dimers was favoured at the molecular level through an extended network of hydrogen-bonded water molecules. The side chains of solvent-accessible residues located at the protein's surface as well as the backbone of the polypeptide chain are less prone to indiscriminate movement since the mean atomic thermal motion is slighter. In the case of insulin, a bound phenolic derivative was detected in earth-grown crystals (Smith *et al.*, 1996), but a second one stabilized by an extensive hydrogen-bonding network mediated by water molecules became visible only in the electron-density map computed from space-grown crystals. This induced a shift towards one protein conformation and displaced its quaternary structure from a trimer to a hexamer (Smith *et al.*, 1995, 1996). These lines of evidence suggest that in the microgravity environment disturbances such as shearing forces that can presumably tear off weakly bound molecules can be minimized. As a consequence, dynamic parts of a protein such as floppy domains or a weakly bound ligand may be 'frozen' in a given state by a network of hydrogen bonds when the crystallization solvent is sufficiently steady.

The positive effect of the reduction in the gravity level appears to be independent of the proportion of solvent in the crystals [43%(*v*/*v*) in lysozyme, 49%(*v*/*v*) in phospholipase A_2 and 62%(*v*/*v*) in AspRS-1 crystals], of the molecular weight of the protein particles (14 300, 140 00 and 122 000 Da, respectively), of space group and packing and of the nature of the crystallizing agent (NaCl, hexanediol and ammonium sulfate, respectively). Our study shows that a large dimeric enzyme that has a flexible structure with floppy loops and extensions such as AspRS-1 behaves like these small and compact proteins in terms of the microgravity positive influence on crystallization.

5. Conclusions

Compared with their equivalent earth-grown counterparts, space-grown AspRS-1 crystals diffract better and have a lower mosaic spread. As a result, an improved initial electron-density map was obtained for modeling and refinement, contributing to clearer structural information on the entire large multidomain enzyme. The improvement seen in the structure of the synthetase dimer was a direct consequence of the enhanced quality of the diffraction data derived from crystals prepared under microgravity.

We thank A. Théobald-Dietrich and D. Kern (Strasbourg) for help and discussions, J. Helliwell (Manchester) for fruitful suggestions and D. Moras (Illkirch) for access to the coordinates of AspRS-1. We express our appreciation to R. Bosch and P. Lautenschlager (Dornier, Friedrichshafen) for their technical support and to O. Minster (ESA, Nordwijk) for administrative support. We acknowledge V. Lamzin and the staff of EMBL at DESY, Hamburg as well as M. Roth and the staff of ESRF, Grenoble for help in synchrotron data collection. We also thank F. van den Akker (Cleveland), Z.-J. Liu (Athens), H. Axelrod (San Diego), C. Kundrot and E. Meehan (Huntsville) for helpful discussions and J. Looger (Huntsville) for technical assistance. This work was supported by the Centre National d'Etudes Spatiales (CNES), the European Space Agency (ESA), the European Community (BIO-CT98-0086), the Centre National de la Recherche Scientifique (CNRS) and University Louis Pasteur (Strasbourg). JDN was

the recipient of an ESA fellowship and CS was supported by MENRT and ARC grants.

References

Akker, F. van den & Hol, W. G. J. (1999). *Acta Cryst.* D**55**, 206–218.
Becker, H. D., Reinbolt, J., Kreutzer, R. & Giegé, R. (1997). *Biochemistry*, **36**, 8785–8797.
Boggon, T. J., Chayen, N. E., Snell, E. H., Dong, J., Lautenschlager, P., Potthast, L., Siddons, D. P., Stojanoff, V., Gordon, E., Thompson, A. W., Zagalsky, P. F., Bi, R. C. & Helliwell, J. R. (1998). *Philos. Trans. R. Soc. London Ser. A*, **356**, 1045–1061.
Borgstahl, G. E. O., Vahedi-Faridi, A., Lovelace, J., Bellamy, H. D. & Snell, E. H. (2001). *Acta Cryst.* D**57**, 1204–1207.
Bosch, R., Lautenschlager, P., Potthast, L. & Stapelmann, J. (1992). *J. Cryst. Growth*, **122**, 310–316.
Briand, C., Poterszman, A., Eiler, S., Webster, G., Thierry, J.-C. & Moras, D. (2000). *J. Mol. Biol.* **299**, 1051–1060.
Broutin-L'Hermite, I., Riès-Kautt, M. & Ducruix, A. (2000). *Acta Cryst.* D**56**, 376–378.
Brünger, A. (1992). *Nature (London)*, **355**, 472–474.
Brünger, A. T., Adams, P. D., Clore, G. M., DeLano, W. L., Gros, P., Grosse-Kunstleve, R. W., Jiang, J. S., Kuszewski, J., Nilges, M., Pannu, N. S., Read, R. J., Rice, L. M., Simonson, T. & Warren, G. L. (1998). *Acta Cryst.* D**54**, 905–921.
Carter, D. C., Lim, K., Ho, J. X., Wright, B. S., Twigg, P. D., Miller, T. Y. Chapman, J., Keeling, K., Ruble, J., Vekilov, P. G., Thomas, B. R., Rosenberger, F. & Chernov, A. A. (1999). *J. Cryst. Growth*, **196**, 623–637.
Colapietro, M., Cappucio, G., Marciante, C., Pifferi, A., Spagna, R. & Helliwell, J. R. (1992). *J. Appl. Cryst.* **25**, 192–194.
Declercq, J.-P., Evrard, C., Carter, D. C., Wright, B. S., Etienne, G. & Parello, J. (1999). *J. Cryst. Growth*, **196**, 595–601.
Delarue, M., Poterszman, A., Nikonov, S., Garber, M., Moras, D. & Thierry, J.-C. (1994). *EMBO J.* **13**, 3219–3229.
DeLucas, L. J. *et al.* (1989). *Science*, **246**, 651–654.
DeLucas, L. J., Long, M. M., Moore, K. M., Harrington, M., McDonald, W. T., Smith, C. D., Bray, T., Lewis, J., Cryssel, W. B. & Weize, L. D. (2000). *Space Technol. Applic. Int. Forum*, **504**, 488–490.
Dong, J., Boggon, T. J., Chayen, N. E., Raftery, J., Bi, R. C. & Helliwell, J. R. (1999). *Acta Cryst.* D**55**, 745–752.
Dong, J., Pan, J., Niu, X., Zhou, Y. & Bi, R. (2000). *Chin. Sci. Bull.* **45**, 1002–1006.
Ducruix, A. & Giegé, R. (1999). Editors. *Crystallization of Nucleic Acids and Proteins. A Practical Approach*, 2nd ed. Oxford: IRL Press.
Evans, S. V. (1993). *J. Mol. Graph.* **11**, 134–138.
Ferrer, J.-L., Hirschler, J., Roth, M. & Fontecilla-Camps, J. (1996). *ESRF Newsl.* **26**, 27–29.
Ferrer, J.-L. & Roth, M. (1998). *J. Appl. Cryst.* **31**, 523–532.
Harp, J. M., Hanson, B. L., Timm, D. E. & Bunick, G. J. (2000). *Acta Cryst.* D**56**, 1513–1534.
Helliwell, J. R. (1988). *J. Cryst. Growth*, **90**, 259–272.
Jones, T. A., Zou, J.-Y., Cowan, S. W. & Kjeldgaard, M. (1991). *Acta Cryst.* A**47**, 110–119.
Kabsch, W. (1988). *J. Appl. Cryst.* **21**, 67–71.
Kleywegt, G. & Jones, A. (1997). *Methods Enzymol.* **277**, 208–230.
Koszelak, S., Day, J., Leja, C., Cudney, R. & McPherson, A. (1995). *Biophys. J.* **69**, 13–19.
Kundrot, C. E., Judge, R. A., Pusey, M. L. & Snell, E. H. (2000). *Cryst. Growth Des.* **1**, 87–99.
Laskowski, R. A., McArthur, M. W., Moss, D. S. & Thornton, J. M. (1993). *J. Appl. Cryst.* **26**, 283–291.
Littke, W. & John, C. (1984). *Science*, **225**, 203–204.
Lorber, B., Sauter, C., Robert, M.-C., Capelle, B. & Giegé, R. (1999). *Acta Cryst.* D**55**, 1491–1494.
McPherson, A. (1982). *Preparation and Analysis of Protein Crystals.* New York: John Wiley & Sons.
McPherson, A. (1996). *Crystallogr. Rev.* **6**, 157–305.
McPherson, A. (1997). *Trends Biotechnol.* **15**, 197–200.
McPherson, A. (1999). *Crystallization of Biological Macromolecules.* Cold Spring Harbor, NY, USA: Cold Spring Harbor Press.
Moore, K. M., Long, M. M. & DeLucas, L. J. (1999). *Space Technol. Applic. Int. Forum*, **458**, 217–224.
Ng, J. D., Lorber, B., Giegé, R., Koszelak, S., Day, J., Greenwood, A. & McPherson, A. (1997). *Acta Cryst.* D**53**, 724–733.
Ng, J. D., Lorber, B., Witz, J., Théobald-Dietrich, A, Kern, D. & Giegé, R. (1996). *J. Cryst. Growth*, **168**, 50–62.
Otálora, F., Capelle, B., Ducruix, A. & Garcia-Ruiz, J. M. (1999). *Acta Cryst.* D**55**, 644–649.
Otálora, F., Novella, M. L., Gavira, J.-A., Thomas, B. R. & Garcia-Ruiz, J. M. (2001). *Acta Cryst.* D**57**, 412–417.
Otwinowski, Z. & Minor, W. (1997). *Methods Enzymol.* **276**, 307–326.
Poterszman, A., Plateau, P., Moras, D., Blanquet, S., Mazauric, M.-H., Kreutzer, R. & Kern, D. (1993). *FEBS Lett.* **325**, 183–186.
Sauter, C., Otálora, F., Gavira, J.-A., Vidal, O., Giegé, R. & Garcia-Ruiz, J. M. (2001). *Acta Cryst.* D**57**, 1119–1126.
Smith, G. D., Ciszak, E. & Pangborn, W. (1995). *Space Technol. Applic. Int. Forum*, **325**, 177–182.
Smith, G. D., Ciszak, E. & Pangborn, W. (1996). *Protein Sci.* **5**, 1502–1511.
Snell, E. H., Weisgerber, S., Helliwell, J. R., Weckert, E., Hölzer, K. & Schroer, K. (1995). *Acta Cryst.* D**51**, 1099–1102.
Vaney, M. C., Maignan, S., Riès-Kautt, M. & Ducruix, A. (1996). *Acta Cryst.* D**52**, 505–517.
Wardell, M. R., Skinner, R., Carter, D. C., Twigg, P. D. & Abrahams, J. P. (1997). *Acta Cryst.* D**53**, 622–625.